

## Modeling catalytic naphtha reforming process using discrete lumping approach

Reza Seif Mohaddecy\* & Sepehr Sadighi

Catalysis and Nanotechnology Research Division, Catalytic Reaction Engineering Department, Research Institute of Petroleum Industry,  
P.O. Box 14665-137, Tehran, Iran

E-mail: seifsr@ripi.ir

Received 29 August 2013; accepted 14 July 2015

Catalytic naphtha reforming is one of key processes in petroleum refineries for improving the octane number of gasoline. Simulation and kinetic modeling of an industrial scale catalytic fixed-bed naphtha reforming plant to predict the important output variables of reforming plant i.e., outlet temperature of three reactors, research octane number, yield of gasoline and hydrogen purity have been studied. The process modeling is based on a discrete-lumped kinetic model consisting twenty-one reaction pathways. All kinetic and deactivation parameters are estimated from pilot plant experiments, and they are fine-tuned using industrial data. To evaluate the simulation, the predicted variables are compared against actual ones. Results show that there is a close mapping between the actual and predicted variables, and the absolute average deviation (AAD%) of the mentioned variables are 0.33, 0.613, 0.689, 0.40, 3.99 and 2.6%, respectively.

**Keywords:** Catalytic naphtha reforming, Modeling, Simulation, Kinetic, Discrete lumping

Catalytic naphtha reforming unit is the heart of modern refineries. This process produces a high-octane liquid product that is rich in aromatic compounds<sup>1,2</sup>. Light gas and liquefied petroleum gas (LPG) are also produced as by-products<sup>3,4</sup>. This process is the main source for hydrogen production as well. In this plant, light petroleum distillate (heavy naphtha) is contacted with a platinum-containing catalyst at elevated temperature and hydrogen pressure. Usually, feed of the catalytic reforming process is heavy straight run naphtha (HSRG), including paraffins, olefins, naphthenes, and aromatics (P.O.N.A) with the carbon number between 5 and 10.

The main reactions of catalytic reforming process are dehydrocyclization, hydrocracking, isomerization, dehydrogenation, and cyclization. Some of these reactions are desired because of increasing octane number of gasoline, and some of them are undesired because of decreasing it. For paraffins, increment of octane number is the result of reactions such as cyclization and aromatization for increasing the number of branches. Therefore, conversion of normal paraffins to isoparaffins, naphthenes, and aromatics increases octane number<sup>5</sup>.

Catalytic reforming process is often modeled based on the: 1. number of reactive species, and 2. type of the used kinetic model. But, presence of many components as reactants or products causes numerous

reactions. Therefore, it extremely makes a sophisticated situation for the process modeling. To decrease these complications, reactants in the mixture are classified into limited groups called pseudo components or lumps. The number of selected lumps in the mixture is a determinant factor for developing the model. Arrhenius and Langmuir-Hinshelwood kinetics are widely used for catalytic reforming models.

In the field of catalytic naphtha process modeling, a simple and first model was suggested by Smith<sup>6</sup> in which naphtha reforming was considered as a combination of only four reactions. Then, in 1997, another model Umesh Taskar suggested a model for catalytic reforming process that was consisted of 35 pseudo components in the reaction network and 36 reactions<sup>7</sup>. Following of using Arrhenius kinetics, a well-known model was proposed by Padmavathi<sup>8</sup> in 1997 in which 26 pseudo components such as alkyl cyclohexane (ACH), alkyl cyclopentane (ACP), normal paraffins (NP), isoparaffins (IP), aromatics (A), hydrogen (H<sub>2</sub>) and light hydrocarbons (C<sub>1</sub> to C<sub>5</sub>) were used in the network. Ancheyta *et al.*<sup>9</sup> developed a kinetic model for the naphtha catalytic reforming process. This model utilized a lumped mathematical, presenting the reactions ranged from 1 to 11 atoms of carbon for paraffins, and from 6 to 11 carbon atoms for naphthenes and aromatics. In 2003, Rahimpour *et al.* presented a kinetic model for an

industrial scale catalytic naphtha reforming plant, in which deactivation of catalyst was also included<sup>10</sup>. The impact of inlet temperature, operating pressure, and catalyst mass distribution on the performance of the reactors was examined. The results indicated that aromatic yield enhanced by increasing the inlet temperature of reactor. But, manipulating the operating pressure had no appreciable effect on the gasoline yield. Additionally, this model estimated catalyst deactivation using the plant data. In 2006, Hou *et al.* proposed a new eighteen-lump kinetic-based mathematical model for an industrial continuous catalytic reforming plant<sup>11</sup>. In this model, reaction temperature and concentration profiles of all reactors, heater duties, catalyst deactivation, recycle gas composition, and octane number for different feedstock or operating conditions were predicted. In the next effort in 2009, Arani *et al.*<sup>12</sup> developed a lumping procedure to obtain kinetic and thermodynamic parameters of a catalytic naphtha reformer using a model consisting of seventeen lumps ranging from C<sub>6</sub> to C<sub>8</sub><sup>+</sup> hydrocarbons, and including fifteen reaction pathways. Moreover, in this year, Fatemi *et al.*<sup>13</sup> developed a mathematical model for a commercial naphtha catalytic reformer, included of three sequencing catalytic fixed-bed reactors at the steady state condition. They used a detailed kinetic scheme involving twenty-six pseudo-components connected by a network including 47 reactions. The output variables of the reformer such as Research Octane Number (RON) and yield of gasoline showed good agreement against actual data obtained from the target reforming unit. Recently, Ziaoon presented a detailed kinetic model including twenty-four components, forming seventy-one reactions<sup>14</sup>. Rahimpour developed a deactivation model for catalytic reforming process using of industrial data<sup>15</sup>. The results of the model show that increasing the reactor weighted average inlet temperature (WAIT) can offset the decrease in aromatic yield. Concentration and temperature profiles have been obtained to provide information about the extent of conversion in the individual reactors.

In this research, a model is proposed for an industrial scale catalytic naphtha reforming plant in which twenty-one hydrocarbons represent feed and product. Additionally, the catalyst deactivation is included in the model. At first, the kinetic parameters of the reforming reactions are obtained from the pilot plant data. Then, these parameters are tuned using data obtained from the industrial scale plant. Using

this model, the important output variables of the industrial reforming plant i.e., outlet temperature of reactors, RON, yield of gasoline, and hydrogen purity are simulated.

## Experimental Section

### Data gathering

The feedstock used in this study was hydrodesulfurized straight-run naphtha obtained from an industrial scale naphtha hydrotreater plant. The feed specifications are presented in Table 1.

The sulfur and water content of hydrodesulfurized naphtha are less than 0.5 and 1 ppm (wt), respectively. The catalyst used in this investigation was a commercial Pt-Re type. The surface area, pore volume, and diameter of that are 221 m<sup>2</sup>/g, 0.36 mL/g and 1.6 mm, respectively.

### Pilot plant experiments

The experiments were carried out in a pilot test system ('Geomecanique BL-2') which is licensed by Institute Francais du Petrole. This device is in the Research Institute of Petroleum Industry (RIPI), and it can tolerate temperatures and pressures up to 500°C and 30 bar, respectively. The simplified diagram of pilot scale catalytic reforming process is presented in Fig. 1. As can be seen, the temperature along the reactor bed is controlled by use of five thermocouples. The flow rate of feed and product are controlled by mass flow controllers. Therefore, an isothermal condition is maintained along the active reactor section.

As can be seen, the feedstock is pumped from the reservoir using a diaphragm metering pump to the top

Table 1—Specification of feed of catalytic naphtha reforming process

Variable	Unit	Value
Specific gravity	-	0.745
Distillation Method (ASTM D86)		
IBP	°C	88
10 % vol	°C	99
30 % vol	°C	105
50 % vol	°C	113
70 % vol	°C	123
90 % vol	°C	137
FBP	°C	156
PONA analysis of feed		
Paraffins	vol %	55
Aromatics	vol %	12
Naphthenes	vol %	33

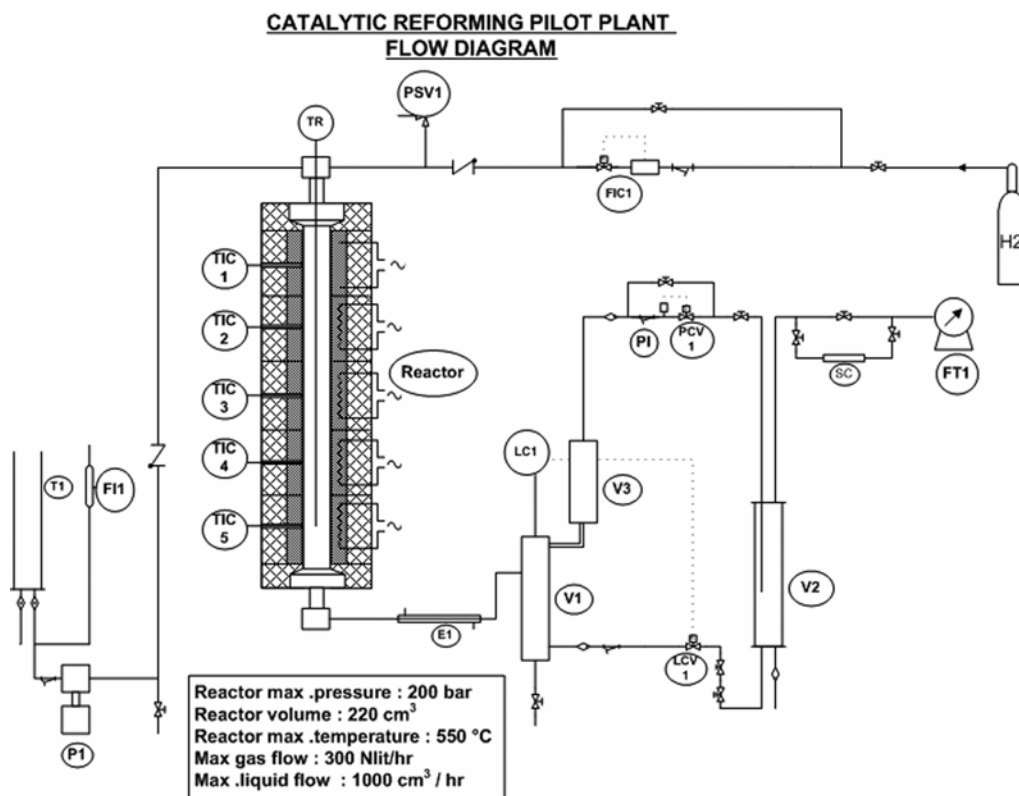


Fig. 1—Schematic diagram of the experimental apparatus catalytic reforming unit

of the reactor. The unit consists of a stainless steel reactor (internal diameter of 1.9 cm and length of 25 cm), kept at isothermal condition using a five-zone electric furnace. In the reactor inlet, the feedstock is mixed with hydrogen, and the temperature of mixture increases to the reaction temperature using the preheating zone of the reactor. Reforming reactions are carried out at the following conditions: (i) Temperature of 450-510°C; (ii) Pressure of 28 bar, and H<sub>2</sub>/hydrocarbon molar ratio of 5-6. As mentioned above, through the bed, there are 5 thermocouples to control the bed temperature. At the reactor outlet, the reaction effluent is cooled using a water-cooled heat exchanger. Then, the vapor and liquid phases are separated in a high pressure separator. After reducing the pressure, the liquid is allowed to flow from the separator to the other flash drum, maintained at atmospheric pressure. The liquid sample is then discharged discontinuously into sampling bottles. Finally, the composition of the gas stream is determined using an online gas chromatograph.

#### Process description of industrial scale plant

An industrial fixed-bed catalytic naphtha reforming unit, called Platformer, licensed by Chevron research

cooperation was chosen as a case study. The feed of the plant prior to entering the catalytic reformer should undergo hydro desulphurization (HDS) reaction in the hydrotreating unit. Then, the produced naphtha, called Platcharge, is introduced to the reforming process<sup>5</sup>.

As shown in Fig. 2, Platcharge is first preheated in the first furnace (H-1), and then it enters the first reactor (R-1) where naphthenes are dehydrogenated to aromatics. Then, the product stream from the first reactor passes through the second reactor (R-2), and the outlet stream of that enters the third reactor (R-3). Most of reforming reactions are endothermic; therefore, a heater should essentially be provided before each reactor (H-1, H-2 and H-3). Next, the product stream from the third reactor enters the flash separator (V-1) wherein the produced hydrogen is separated, and recycled to the beginning of the process. This stream is then mixed with the fresh naphtha feed (Platcharge). Finally, the liquid product leaving the separator is introduced to the gasoline stabilizer in which the LPG and light gases are separated from the gasoline. So, the vapour pressure of the gasoline can be set according to the market requirement.

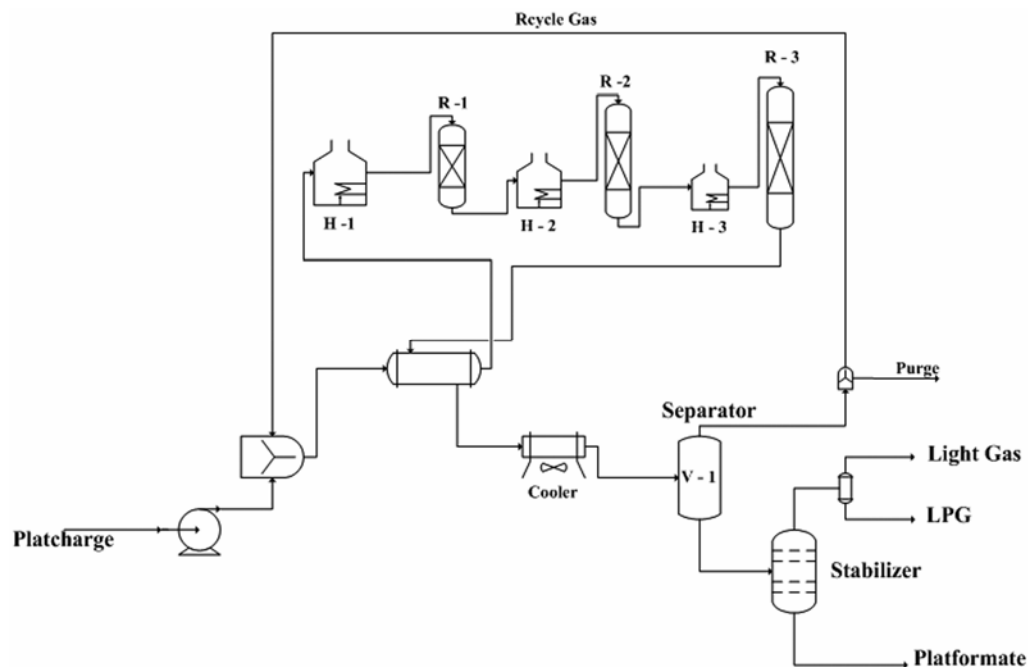


Fig. 2—Catalytic reforming flowchart (Semi-Regenerative)

The specifications of feed, catalyst distribution and normal operating conditions of the unit are presented Tables 1 and 2.

The design pressure of the target catalytic reforming plant is 34 bar. But, dependent to the feed specification and the deactivation rate of the catalyst, the pressure can be varied between 27 and 32 bar. So, the effect of the pressure on reforming reactions should be included in the model, discussed later.

#### Model development

##### Reaction model

Chemical components taking part in the catalytic reforming system are more than 300 species, measurable by using gas chromatography method<sup>5</sup>. Developing the model for this complex system is extremely difficult. But, the large number of chemical components can be reduced to a manageable set of kinetic lumps, each composed of chemical species which have sufficiently similar characteristics<sup>8-13</sup>.

As mentioned before, the feed of reforming plant is a hydrotreated straight run heavy naphtha, consisting naphthenic groups i.e., alkyl cyclohexanes ( $ACH_n$ ) and alkyl cyclopentanes ( $ACP_n$ ), paraffinic group i.e., normal paraffins ( $NP_n$ ) and isoparaffins ( $IP_n$ ), and aromatics ( $An$ ). In this research, they are identified as discrete-lumps including  $C_6$  to  $C_9$  hydrocarbons. In addition, methane, ethane, propane, butane, and pentane are the light gas of this network.

Table 2—Catalyst distribution and operating conditions in the catalytic reforming of the target oil refinery

	1st reactor	2nd reactor	3rd reactor
Catalyst weight (kg)	8648	14223	22452
Catalyst distribution (wt %)	20	30	50
Process Variable		Unit	Value
Inlet temperature		°C	490-515
Hydrogen/hydrocarbon ratio		mol/mol	3-7
Space Velocity		$h^{-1}$	1- 2
Yield		vol %	70 - 85

Figure 3 demonstrates the reaction network proposed in this research with 21 pseudo components or lumps for modeling the target catalytic reformer, including carbon fractions up to  $C_9$  for covering reactions occurring through the catalytic bed of reforming plant. According to the Fig. 3, reaction rates can be written as follows:

ACH dehydrogenation

$$ACH_n \longleftrightarrow A_n + 3H_2 \quad \frac{dX_{1n}}{d\theta} = k_{1n} (P_{ACHn} - \frac{P_{An} P_{H_2}^3}{K_{1n}}) = r_{1n} \quad \dots(1)$$

Ring Expansion

$$ACP_n \longleftrightarrow ACH_n \quad \frac{dX_{2n}}{d\theta} = k_{2n} (P_{ACPn} - \frac{P_{ACHn}}{K_{2n}}) = r_{2n} \quad \dots(2)$$

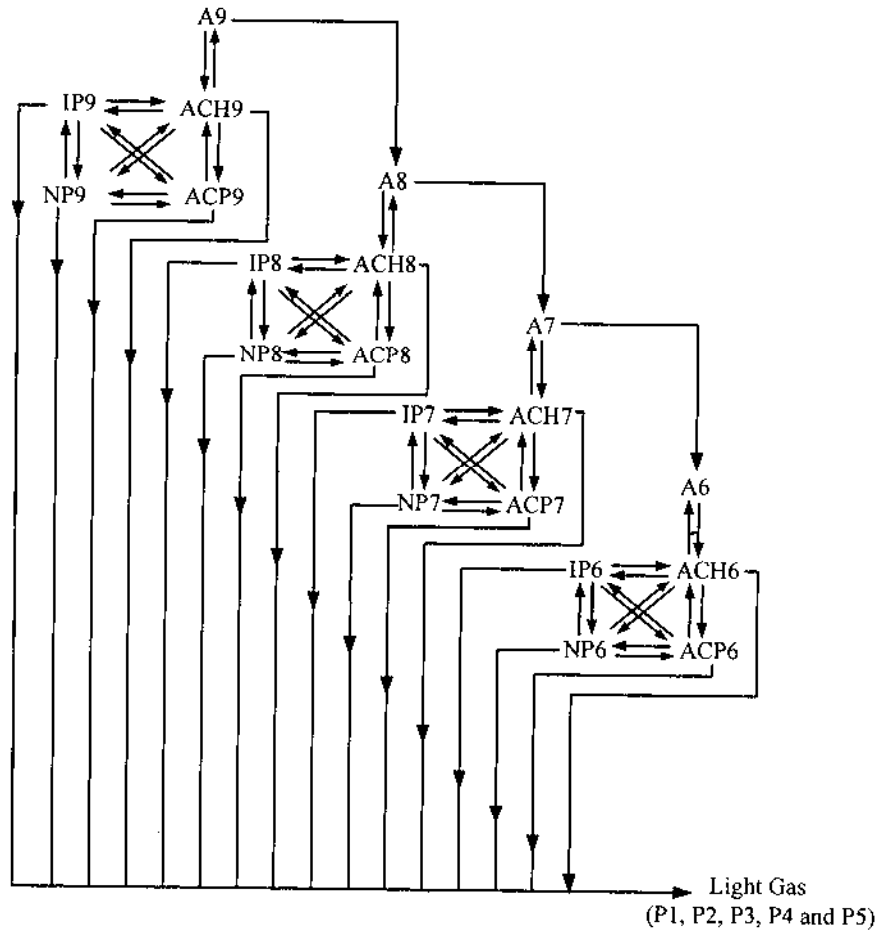


Fig. 3—Reaction network for catalytic reforming reactions

ACH Hydrogenation

$$ACH_n + H_2 \longleftrightarrow NP_n \quad \frac{dX_{3n}}{d\theta} = k_{3n} (P_{ACHn} P_{H_2} - \frac{P_{NPn}}{K_{3n}}) = r_{3n} \quad \dots(3)$$

$$ACH_n + H_2 \longleftrightarrow IP_n \quad \frac{dX_{4n}}{d\theta} = k_{4n} (P_{ACHn} P_{H_2} - \frac{P_{IPn}}{K_{4n}}) = r_{4n} \quad \dots(4)$$

Normal paraffins dehydrogenation

$$NP_n \longleftrightarrow ACP_n + H_2 \quad \frac{dX_{5n}}{d\theta} = k_{5n} (P_{NPn} - \frac{P_{ACHn} P_{H_2}}{K_{5n}}) = r_{5n} \quad \dots(5)$$

Iso paraffins dehydrogenation

$$IP_n \longleftrightarrow ACP_n + H_2 \quad \frac{dX_{6n}}{d\theta} = k_{6n} (P_{IPn} - \frac{P_{ACPn} P_{H_2}}{K_{6n}}) = r_{6n} \quad \dots(6)$$

Normal paraffins isomerization

$$NP_n \longleftrightarrow IP_n \quad \frac{dX_{7n}}{d\theta} = k_{7n} (P_{NPn} - \frac{P_{IPn}}{K_{7n}}) = r_{7n} \quad \dots(7)$$

Normal paraffins hydrocracking

$$NP_n + \frac{n-3}{3} H_2 \longrightarrow \sum_{i=1}^5 C_i \quad \frac{dX_{8n}}{d\theta} = k_{8n} (\frac{P_{NPn}}{P_t}) = r_{8n} \quad \dots(8)$$

Iso paraffins hydrocracking

$$IP_n + \frac{n-3}{3} H_2 \longrightarrow \sum_{i=1}^5 C_i \quad \frac{dX_{9n}}{d\theta} = k_{9n} (\frac{P_{NPn}}{P_t}) = r_{9n} \quad \dots(9)$$

ACH hydrocracking

$$ACH_n + \frac{n}{3} H_2 \longrightarrow \sum_{i=1}^5 C_i \quad \frac{dX_{10n}}{d\theta} = k_{10n} (\frac{P_{ACHn}}{P_t}) = r_{10n} \quad \dots(10)$$

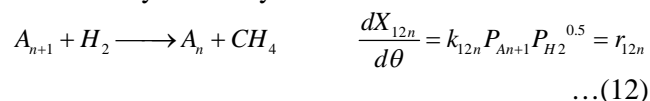
ACP hydrocracking

$$ACP_n + \frac{n}{3} H_2 \longrightarrow \sum_{i=1}^5 C_i \quad \frac{dX_{11n}}{d\theta} = k_{11n} (\frac{P_{ACPn}}{P_t}) = r_{11n} \quad \dots(11)$$

A kinetic study of a reaction can be simplified by running the reaction with one or more of the

components in large excess, so that the concentration remains effectively constant. In hydrocracking reaction (Eqs 7-11), hydrogen is an excess of component, and its concentration remains constant, so that the rate equation of hydrocracking is independent of hydrogen concentration. [Eqs 6, 8, 9, 10, 11]

Aromatic hydrodealkylation



Where  $k$ ,  $K$  and  $P_i$  are rate constant, equilibrium constant and partial pressure.

Arrhenius rate expression is applied to describe the rate of each reaction<sup>8</sup>. Therefore, the rate constant concerning above reactions is as follows:

$$k_{in} = k_0 e^{\frac{-E}{RT}} \quad \dots (13)$$

where  $k_0$  and  $E$  are pre-exponential factor and activation energy, respectively.

#### Deactivation model

The activity of a catalyst is the ability to increase the rate of reactions measured by the temperature at which the catalyst should be operated to produce a product with the desired specifications whilst all other operating conditions are kept constant. Reforming catalysts are temporarily deactivated due to the coke deposition, burnt in the regenerator during the regeneration process.

A comprehensive model should accurately predict the rate of coke formation, in consequence with catalyst deactivation versus days on stream (DOS). To develop such a model, the rate equations are reformulated by introducing the catalyst activity ( $a$ ) as follows<sup>8</sup>:

$$r_i(t) = r_i(0) \cdot a \quad 0 \leq a \leq 1 \quad \dots(14)$$

where  $r_i(0)$  is the reaction rate at the start of run when there is no coke on the catalyst;  $r_i(t)$  is the rate of reaction at time  $t$ , and  $a$  is the activity of catalyst. The latter depends on the reaction temperature, coke content and cycle time. Accordingly, it is the ratio of reaction rate at any time ( $t > 0$ ) to the reaction rate at the start of run ( $t = 0$ ) as follows:

$$a(t) = \frac{(Rate)_t}{(Rate)_{t=0}} \quad \dots(15)$$

The deactivation model employed in this research is as the following<sup>15</sup>:

$$\frac{da}{dt} = -K_d \exp\left(\frac{-E_d}{R} \left(\frac{1}{T} - \frac{1}{T_R}\right)\right) a^m \quad \dots(16)$$

where  $k_d$ ,  $E_d$  and  $m$  are model parameters determined using industrial plant data, and  $T_R$  is the reference temperature (770 K). In Eq.15, where  $r(0)$  is the reaction rate at the start of a cycle when the catalyst is fresh and  $r(t)$  is the rate of reaction at time  $t$ . This deactivation model includes three parameters,  $k_d$ ,  $E_d$  and  $m$ , that are determined using industrial plant data. The reactor is divided into several weight intervals such that in each interval the amount of catalyst activity is constant and is function of time and catalyst temperature. Reaction rate in each interval is obtained by Eq. 15 and is then used in material and energy balance equations (Eqs 17-26).

#### Reactor modeling

The model of reactor consists of differential equations representing the mass and energy conservations. Ergun's equation for calculating the pressure drop is also included in the differential format, integrated with the other equations. Moreover,

Peng-Robinson (PR) equation of state is applied to describe the thermodynamic equilibrium of hydrocarbon mixtures. Therefore, using the proposed rate equations, the model of reactor can be represented as follows:

$$\frac{dX_{ACP}^n}{d\theta} = -r2_n + r5_n + r6_n - r11_n \quad \dots (17)$$

$$\frac{dX_{ACH}^n}{d\theta} = -r1_n + r2_n - r3_n - r4_n - r10_n \quad \dots (18)$$

$$\frac{dX_{IP}^n}{d\theta} = r4_n - r6_n + r7_n - r9_n \quad \dots (19)$$

$$\frac{dX_{A6}}{d\theta} = r1_6 + r12_6 \quad \dots (20)$$

$$\frac{dX_{A7}}{d\theta} = r1_7 - r12_6 + r12_7 \quad \dots (21)$$

$$\frac{dX_{A8}}{d\theta} = r1_8 - r12_7 + r12_8 \quad \dots (23)$$

$$\frac{dX_{A9}}{d\theta} = r_{19} - r_{128} \quad \dots (24)$$

$$\frac{dX_{H2n}}{d\theta} = 3r_{1n} - r_{3n} - r_{4n} + r_{5n} + r_{6n} - \frac{n-3}{3}(r_{8n} + r_{9n}) - \frac{n}{3}(r_{10n} + r_{11n}) - r_{12n} \quad \dots (25)$$

$$\frac{dT}{d\theta} = \sum_{n=6}^9 \left( \sum_{i=1}^{12} (-\Delta H_{i_n}) r_{i_n} \right) \frac{F}{\sum_j F_j C_{p_j}} \quad \dots (26)$$

$$\frac{dP}{dW} = -\frac{G}{\rho d_p \phi^3} \left( \frac{150(1-\phi)\mu}{d_p} + 1.75G \right) \frac{1}{A_c \rho_c} \quad \dots (27)$$

**Calculation of RON**

Research Octane number (RON) is a standard measure of the performance of a motor or aviation fuel. The higher the octane number, the more compression the fuel can withstand before detonating. In broad terms, fuels with a higher octane rating are used in high-compression engines that generally have higher performance. Use of gasoline with lower octane numbers may lead to the problem of engine knocking. RON is determined by running the fuel in a test engine with a variable compression ratio under controlled conditions, and comparing the results with those for mixtures of iso-octane and *n*-heptane.

RON of gasoline can be directly measured by standard CFR engine (ASTM D2699). But, this test is relatively expensive. In the new calculation method proposed by the researchers, a non-linear equation for the prediction of RON is regressed as follows:

$$RON = a + b\left(\frac{T_b}{100}\right) + c\left(\frac{T_b}{100}\right)^2 + d\left(\frac{T_b}{100}\right)^3 + e\left(\frac{T_b}{100}\right)^4 \quad \dots (28)$$

where  $T_b$  is the normal boiling point (°C), and the regression coefficients (a,b,c,d and e) are available for pure components<sup>16</sup>. So, to estimate the RON of a mixture, the following equation can be applied<sup>17</sup>:

$$RON = \sum_{i=1}^n RON_i y_i \quad \dots (29)$$

where  $y_i$  is volume fractions of hydrocarbons present in the gasoline, measured by GC, and  $RON_i$  is the octane of pure components in the gasoline mixture.

**Model development**

At first, the apparent parameters of the kinetic models such as activation energy and pre-exponential factor of reactions were determined using data obtained from the pilot-scale. Then, pre-exponential factors, activation energies, and deactivation parameters of the proposed model were determined using data obtained from the industrial scale plant. The minimization of the objective function, based on the sum of squared errors between experimental and model values, was applied to find the best set of kinetic parameters. This objective function was solved using the least squares criterion with a nonlinear regression procedure based on Marquardt's algorithm [18].

$$f = \sum_{i=1}^n (0.5(C_{i_{exp}} - C_{i_{model}})^2 + 0.5(T_{i_{exp}} - T_{i_{model}})^2) \quad \dots (30)$$

Thereafter, the modified 21-lump kinetic based model is extended as a user module in Aspen-Hysys software (Ver. 2010) to simulate the catalytic reforming plant. The steps to design this user module are as follows:

- (i) The reactor model including the 21-lump kinetic model is developed as a subroutine in VBA (visual basic application) Ver. 2012.
- (ii) The subroutine is compiled into an object file or a shared library by the visual basic compiler.
- (iii) The object file or shared library is copied to the working directory and distributed to Aspen-Hysys platform.
- (iv) A user module is selected on the Aspen-Hysys user interface. Then, the subroutine is loaded automatically when the user module is simulated.
- (v) Other equipment such as heaters, flash drum, stabilizer column and heat exchanger are simulated using the available modules in aspen-hysys environment.
- (vi) The input parameters, calculation results and important inner information such as temperature and reformat composition profiles within the three reactors are introduced as output in the report file.

**Results and Discussions**

To identify the activity of the catalyst, seventeen data points during 330 days for three different reactor temperatures were obtained from the target plant (Table 3). All data were selected from the normal

Table 3—Product RON of industrial catalytic reforming plant

No.	Time (h)	Product RON		
		Reactor temp. 785 K	Reactor temp. 765 K	Reactor temp. 7450 K
1	0	105	100	96.5
2	500	101	98.5	95
3	1000	98	97	94
4	1500	95	96	93
5	2000	93.5	94.5	92.5
6	2500	91.5	93	91.7
7	3000	89	92.5	91
8	3500	88	91.5	90
9	4000	87	90	89
10	4500	86	88.5	88.5
11	5000	85	88	88
12	5500	84	87.5	87.5
13	6000	83	87	87
14	6500	82.5	85.5	86.5
15	7000	81.5	84	86
16	7500	81	83.5	85
17	8000	80	82.5	84

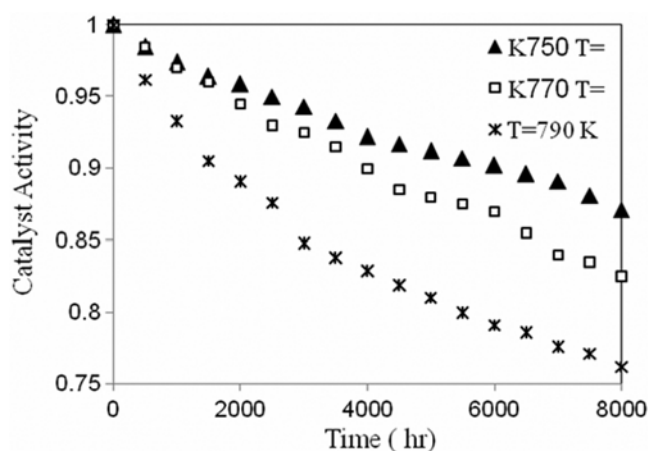


Fig. 4—Catalyst activity calculated for target catalytic reforming unit in different operation temperatures.

condition when no abnormalities such as tower flooding, emergency depressurization, and pump or compressor shut down were happen in the operation. The catalyst activity calculated based on RON of product are shown in Fig. 4. Using the catalyst activity presented in Fig. 4, deactivation parameters of the proposed model were determined (Table 4).

To determine the kinetic parameters of catalytic reforming process, ninety six data points based on experimental design procedure were obtained from the pilot plant. The estimated parameters are presented in Table 5. For validating the kinetic and

Table 4—Deactivation model Parameters

$K_d$	$E_d$	$m$
0.000037	21813.5	5

deactivation model, ten sets of data were obtained from the industrial scale plant (Table 6). Then, to evaluate the accuracy of the model, the simulated data are compared with the actual (industrial) ones.

Figure 5 show comparisons between the outlet reactor temperatures obtained by the model against the actual values. Results show that AAD% of the predicted temperatures are 0.33, 0.613, and 0.709%, respectively. As can be seen, close mappings between the measured and simulated outlet temperatures of reactors can be understood.

The most important variable in the catalytic reforming are product volume yield and research octane number (RON). The RON of gasoline depends on the types of hydrocarbons present in the mixture. Comparison of the predicted RON based on equation 29 with the actual data is shown in Fig. 6. From this figure, it is found that the presented model can simulate the RON of the gasoline with the AAD% of 0.318%. This result confirms that the presented approach can be reliably applied by refineries to monitor the operation of the catalytic reforming plant.

The other significant controlled variables in the catalytic reforming plant are the hydrogen purity of



Table 5—Reaction constants calculated using optimized approach

No.	Reaction	$k_0$	E
1	NP <sub>5</sub> to IP <sub>5</sub>	2.572E+14	51667
2	IP <sub>5</sub> to NP <sub>5</sub>	2.803E+13	51664
3	IP <sub>5</sub> hydrocracking	1.776E+3	68000
4	NP <sub>5</sub> hydrocracking	5.000E+01	68000
5	ACH <sub>6</sub> to A <sub>6</sub>	1.1793E+11	38751
6	A <sub>6</sub> to ACH <sub>6</sub>	6.45E+01	19.5
7	ACP <sub>6</sub> to ACH <sub>6</sub>	1.97E+13	47315
8	ACH <sub>6</sub> to ACP <sub>6</sub>	1.58E+14	51664
9	ACH <sub>6</sub> to NP <sub>6</sub>	2.857E+13	65796
10	NP <sub>6</sub> to ACH <sub>6</sub>	3.3196E+17	76225
11	ACH <sub>6</sub> to IP <sub>6</sub>	2.090E+14	65796
12	IP <sub>6</sub> to ACH <sub>6</sub>	1.734E+19	78761
13	ACH <sub>6</sub> hydrocracking	1.2958E+21	68777
14	ACP <sub>6</sub> to NP <sub>6</sub>	2.0539E+13	65793
15	NP <sub>6</sub> to ACP <sub>6</sub>	3.1412E+15	65796
16	ACP <sub>6</sub> to IP <sub>6</sub>	3.1412E+16	65796
17	IP <sub>6</sub> to ACP <sub>6</sub>	2.857E+13	65793
18	ACP <sub>6</sub> hydrocracking	1.2958E+21	68777
19	NP <sub>6</sub> to IP <sub>6</sub>	3.1892E+13	51667
20	IP <sub>6</sub> to NP <sub>6</sub>	3.2620E+12	51664
21	NP <sub>6</sub> hydrocracking	2.3671E+21	68777
22	A <sub>7</sub> to A <sub>6</sub>	1.9551E+06	35611
23	IP <sub>6</sub> hydrocracking	2.8912E+22	68777
24	ACH <sub>7</sub> to A <sub>7</sub>	1.9059E+12	38700
25	A <sub>7</sub> to ACH <sub>7</sub>	9.24E+01	19.5
26	ACP <sub>7</sub> to ACH <sub>7</sub>	1.9734E+13	47310
27	ACH <sub>7</sub> to ACP <sub>7</sub>	1.58E+14	51664
28	ACH <sub>7</sub> to NP <sub>7</sub>	3.03337E+13	65796
29	NP <sub>7</sub> to ACH <sub>7</sub>	1.0896E+18	73910
30	ACH <sub>7</sub> to IP <sub>7</sub>	3.118E+14	65796
31	IP <sub>7</sub> to ACH <sub>7</sub>	1.34E+20	76141
32	ACH <sub>7</sub> hydrocracking	2.1363E+21	68777
33	ACP <sub>7</sub> to NP <sub>7</sub>	2.5087E+13	65793
34	NP <sub>7</sub> to ACP <sub>7</sub>	3.335E+15	65796
35	ACP <sub>7</sub> to IP <sub>7</sub>	3.3355E+15	65796
36	IP <sub>7</sub> to ACP <sub>7</sub>	3.0337E+13	65793
37	ACP <sub>7</sub> hydrocracking	1.2958E+21	68777
38	NP <sub>7</sub> to IP <sub>7</sub>	3.1892E+13	51667
39	IP <sub>7</sub> to NP <sub>7</sub>	3.2620E+12	51664
40	NP <sub>7</sub> hydrocracking	2.8912E+21	68777
41	A <sub>8</sub> to A <sub>7</sub>	1.9551E+06	35611

(Contd.)

Table 5—Reaction constants calculated using optimized approach (*contd.*)

No.	Reaction	$k_0$	E/R
42	IP <sub>7</sub> hydrocracking	3.5314E+22	68777
43	ACH <sub>8</sub> to A <sub>8</sub>	22591E+12	38000
44	A <sub>8</sub> to ACH <sub>8</sub>	1.634E+01	19.5
45	ACP <sub>8</sub> to ACH <sub>8</sub>	1.97E+13	47315
46	ACH <sub>8</sub> to ACP <sub>8</sub>	1.58E+14	51664
47	ACH <sub>8</sub> to NP <sub>8</sub>	7.295E+13	65796
48	NP <sub>8</sub> to ACH <sub>8</sub>	2.8314E+19	74968
49	ACH <sub>8</sub> to IP <sub>8</sub>	2.814E+15	65796
50	IP <sub>8</sub> to ACH <sub>8</sub>	2.267E+21	76721
51	ACH <sub>8</sub> Hydrocracking	5.8072E+21	68777
52	ACP <sub>8</sub> to NP <sub>8</sub>	6.7516E+13	65793
53	NP <sub>8</sub> to ACP <sub>8</sub>	2.9506E+17	65796
54	ACP <sub>8</sub> to IP <sub>8</sub>	3.1646E+18	65796
55	IP <sub>8</sub> to ACP <sub>8</sub>	7.2950E+14	65793
56	ACP <sub>8</sub> hydrocracking	1.2957E+21	68777
57	NP <sub>8</sub> to IP <sub>8</sub>	4.7578E+15	51667
58	IP <sub>8</sub> to NP <sub>8</sub>	3.2620E+10	51664
59	NP <sub>8</sub> hydrocracking	3.1953E+21	68777
60	A <sub>8</sub> to A <sub>7</sub>	1.9551E+06	35611
61	IP <sub>8</sub> hydrocracking	3.1953E+21	68777
62	ACH <sub>9</sub> to A <sub>9</sub>	5.2854E+12	38750
63	A <sub>9</sub> to ACH <sub>9</sub>	2.12E+01	19.5
64	ACP <sub>9</sub> to ACH <sub>9</sub>	1.97E+13	47315
65	ACH <sub>9</sub> to ACP <sub>9</sub>	1.58E+14	51664
66	ACH <sub>9</sub> to NP <sub>9</sub>	6.2627E+13	65796
67	NP <sub>9</sub> to ACH <sub>9</sub>	2.0868E+20	74689
68	ACH <sub>9</sub> to IP <sub>9</sub>	6.2627E+15	65796
69	IP <sub>9</sub> to ACH <sub>9</sub>	4.6310E+20	76294
70	ACH <sub>9</sub> Hydrocracking	9.5744E+21	68777
71	ACP <sub>9</sub> to NP <sub>9</sub>	4.8413E+14	65793
72	NP <sub>9</sub> to ACP <sub>9</sub>	1.5364E+18	65796
73	ACP <sub>9</sub> to IP <sub>9</sub>	1.5364E+19	65796
74	IP <sub>9</sub> to ACP <sub>9</sub>	6.2626E+15	65793
75	ACP <sub>9</sub> hydrocracking	1.2958E+21	68777
76	NP <sub>9</sub> to IP <sub>9</sub>	4.7578E+13	51667
77	IP <sub>9</sub> to NP <sub>9</sub>	3.2620E+12	51664
78	NP <sub>9</sub> hydrocracking	2.1363E+22	68777
79	A <sub>9</sub> to A <sub>8</sub>	1.9551E+06	35611
80	IP <sub>9</sub> hydrocracking	2.1363E+22	68777

Table 6—Operation Condition of actual test run of target catalytic reforming unit

Variable	Unit	Test Run 1	Test Run 2	Test Run 3	Test Run 4	Test Run 5
Days on stream	day	95	123	158	179	195
H <sub>2</sub> to hydrocarbon ratio	mol / mol	5.32	5.58	5.22	4.97	5.0
Feed flow rate	kg/ hr	74109	73111	73111	73824	73824
First reactor inlet temp.	°C	499.44	500.56	501.11	500	499.5
First reactor inlet temp.	°C	499.44	500.56	501.11	499.44	500
First reactor inlet temp.	°C	499.44	500.56	501.11	501.11	500
Separator temp.	°C	37.78	37.78	37.78	37.78	37.78

*(Contd.)*

Table 6—Operation Condition of actual test run of target catalytic reforming unit (Contd.)

Variable	Unit	Test Run 6	Test Run 7	Test Run 8	Test Run 9	Test Run 10
Days on stream	day	245	310	390	450	530
H <sub>2</sub> to hydrocarbon ratio	mol / mol	5.1	5.1	5.1	5.1	5.1
Feed flow rate	kg/ hr	73824	73824	73824	73824	73824
First reactor inlet temp.	°C	500.12	501.2	501	502.3	502
First reactor inlet temp.	°C	500.12	501.2	501	502.3	502
First reactor inlet temp.	°C	500.12	501.2	501	502.3	502.8
Separator temp.	°C	37.78	37.78	37.78	37.78	37.78

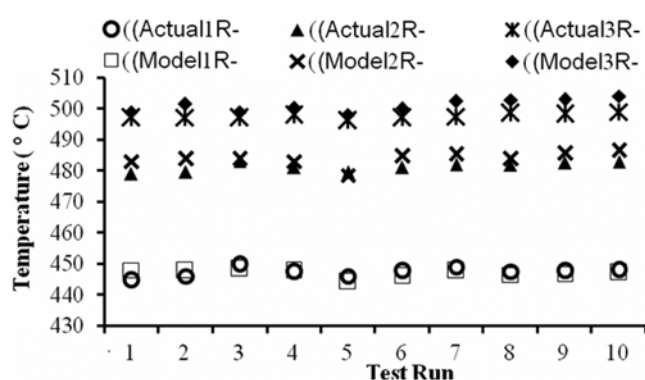
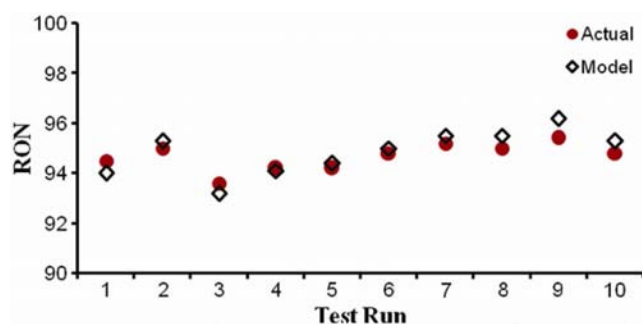

 Fig. 5—Simulated outlet temperature of 1<sup>st</sup>, 2<sup>nd</sup>, 3<sup>rd</sup> reactors (R-1, R-2, R-3) against actual values


Fig. 6—Simulated RON of product against actual values

the recycle stream and product volume yield. In Figs 7 and 8, the comparisons between the simulated hydrogen purity and product volume yield with the actual data are presented. These results show that the kinetic model can predict the purity of the produced hydrogen and product volume yield with the AAD% of 2.6 and 3.99%, respectively. It is concluded that the presented kinetic model is reliable for predicting the purity of hydrogen product and gasoline volume yield as well.

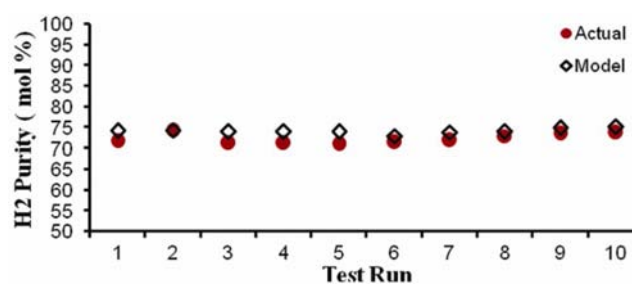


Fig. 7—Simulated hydrogen purity (mole%) against actual values

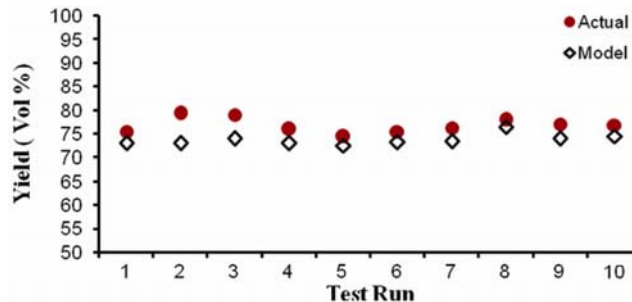


Fig. 8—Simulated volume yield of gasoline against actual values

## Conclusions

The catalytic reforming of heavy naphtha is a favourite process in petroleum refineries due to producing high octane number gasoline. In this research, significant process variables of a commercial naphtha catalytic reforming plant are predicted using a discrete-lumped kinetic model. These variables are outlet temperatures of the first, second and third reactors, RON of gasoline, product volume yield and hydrogen purity. To evaluate the proposed model, results are compared against data obtained from a commercial catalytic naphtha reformer. It has been found that the AAD% of the mentioned parameters are 0.33, 0.613, 0.689, 0.4, 3.99 and 2.6%, respectively. Therefore, a close mapping between the simulated variables and data

obtained from an industrial-scale reforming plant is confirmed. These results show that the presented kinetic model can reliably be utilized to monitor the operation of the catalytic reforming plant.

### Nomenclature

$X_{in}$	= Conversion by reaction i for the carbon number n
$\theta$	= kg catalyst / (kmol/h)
$r_{in}$	= reaction rate, kmol/kgcatalyst.h
$k_{in}$	= rate constant, variable dimensions
$P_i$	= Partial pressure, Kpa
$K_{in}$	= Equilibrium constant, variable dimension
$k_0$	= Pre-exponential factor, variable dimensions
$E$	= Activation Energy, kcal /kmol
$T$	= Inlet Temperature, K
$R$	= Gas constant, 1.9872 kcal/kmol.K
$a$	= Catalyst activity, dimensionless
$r_i(0)$	= Reaction rate at the start of run
$r_i(t)$	= Rate of reaction at time t
$k_d$	= Deactivation model parameter, hr <sup>-1</sup>
$E_d$	= Deactivation model parameter, kcal/kmol
$m$	= Deactivation model parameter, dimensionless
$y_i$	= Volume fraction of gasoline components
$\Delta H$	= Heat of Reaction, kcal/kmol
$F$	= Feed flow rate, kmol/h
$F_j$	= Flow rate of j th component, kmol/h
$C_{pj}$	= Heat Capacity of jth component, kcal/kmol ° K
$P$	= Total pressure, Kpa
$W$	= catalyst weight, kg
$G$	= Superficial mass flux, kg / sec m <sup>2</sup>
$\rho$	= Density of gases mixture, kg / m <sup>3</sup>
$d_p$	= Catalyst particle diameter, m
$\phi$	= Bed void fraction,

$\mu$	= Viscosity of the gas, kg / mSec
$A_c$	= Cross section of flow in the reactor, m <sup>2</sup>
$\rho_c$	= catalyst Density, kg / m <sup>3</sup>
SOR	= Start of run
EOR	= End of run
RON	= Research octane number
$y_i$	= Volume fraction of gasoline components
AAD	= Absolute average deviation

### References

- 1 Pieck C L, Carlos R V, Parera M, Gustavo N G, Luciano R S, Luciene S C & Maria C R, *J Catal Today*, 107 (2005) 637.
- 2 Silvana A D, Carlos R V, Florence E, Catherine E, Patrice M & Carlos L P, *J Catal Today*, 133 (2009) 13.
- 3 Chang A, Pashikanti K & Liu Y A, *Refinery Engineering*, (John Wiley & Sons) 2012.
- 4 Fahim M A, Al-Sahhaf T A & Elkilani A, *Fundamentals of Petroleum Refining*, (Elsevier) 2009.
- 5 Antons G A & Aitani A M, *Catalytic Naphtha Reforming*, (Marcel Dekker Inc), 2004.
- 6 Smith R B, *Chem Eng Prog*, 55 (1959) 76.
- 7 Taskar U, *AIChE J*, 43 (1997) 740.
- 8 Padmavathi G & Chaudhuri K K, *Canadian J Chem Eng*, 75 (1997) 930.
- 9 Ancheyta J & Villafuerte E, *Energy Fuels*, 14 (2000) 1032.
- 10 Rahimpour M R, Esmaili S & Bagheri G N A, *Iran J Sci Technol, Trans B: Tech*, 27 (2003) 279.
- 11 Hou W, Su H & Chu J, *Chinese J Chem Eng*, 14 (2006) 584.
- 12 Arani H M, Shirvani M, Safdarian K & Dorostkar E, *Brazilian J Chem Eng*, 26 (2009) 723.
- 13 Fazeli A, Fatemi S, Mahdavian M & Ghaee A, *Iran J Chem Chem Eng*, 28 (2009) 97.
- 14 Zaidoon M, *Diyala J Eng Sci*, 4 (2011) 86.
- 15 Rahimpour M R, *Chem Eng Technol*, 29 (2006) 616.
- 16 Albahri A, Riazi M R & Alqattan A A, *Fuel Chemistry Division Preprints*, 47 (2002) 710.
- 17 Nikolaou V, Papadopoulou C E, Gagliasb I A & Pitarakisc K G, *Fuel*, 83 (2004) 517.
- 18 Marquardt D W, *J Soc Indust Appl Math*, 2 (1963) 431.